Research Paper

Experimental and Theoretical Study on Screwed Connections in Cold-Formed Steel Structure

Rattanasak HONGTHONG[1)], Apai BENCHAPHONG[1)]
Sutera BENCHANUKROM[2)], Nirut KONKONG[3)]

[1)] *Department of Civil Engineering, Faculty of Engineering*
Rajamangala University of Technology
Krungthep, 10120, Thailand

[2)] *Department of Industrial Construction Technology*
Faculty of Agricultural Technology and Industrial Technology
Phetchabun Rajabhat University
Phetchabun, Thailand

[3)] *P.A.I.R Engineering Co., Ltd*
Bangkok, 10210, Thailand
Corresponding Author e-mail: Nirut Konkong: nirut.k@ku.th

This research aims to study the fastening rotation behavior of cold-formed steel screw connections by experimental testing and analytical modelling. Both the experimental test and finite element results showed the failure modes of tilting and bearing failure. The rotation failure mode of the screw connection was studied by an analytical method using a spring model with screw-plate stiffness which included the bending and shear stiffness of the screw and the bearing stiffness of the screw and plates. Variation in the screw thread diameter, plate thickness, and plate thickness ratio are assigned to the spring model for the parametric study. The screw rotation or tilting was primarily controlled by the plate thickness. Presented results show that to decrease the effect of tilting failure, the end of the screw should be embedded within the thickest side of the cold-formed steel parts.

Key words: cold-formed steel; lap shear test; finite element analysis; analytical method; screw-plate stiffness.

1. Introduction

Cold-formed steel is widely used in the building and construction industry. This popularity is due to the characteristics of cold-formed steel structures as being lightweight structures, with low cost of transportation, and simple installation [1, 2]. Additionally, cold-formed steel is non-flammable and has a minimal risk of deformation and failure during and after high-temperature fires [3, 4].

The connections between structural components in a cold-formed steel structure are of great importance, as their function is to transfer loads from one member to another. A variety of assembly methods; clinching, welding, using structural adhesives, screws, steel pin rivets, staples, and pallet rack connections, are used in cold-formed steel connections [5–7]. Due to the thin thickness of a cold-formed steel, screws are a common type of connection used. Screw connections are also simple designs, allowing fast installation, and are self-drilling, making screw connections highly advantageous. The behavior of self-drilling screws was discussed in [8] as showing excellent moment capacity and connection rigidity. An important advantage of screw connections, among others, is that it can be loaded by applying multi-directional force where the tension load is always parallel to the normal axis and the shear load is always perpendicular to this axis of the screw. The direction of the load depends on the type of the connecting structural elements; overlap or moment connection [9]. The failure mode of a single overlap screw connection can be a gross cross-section failure, net cross-section fracture, pull-out, bearing, tilting, combined bearing-tilting and screw shear [10–15]. In AISI-2015 [16], the nominal shear strength (P_{ns}) of tilting and bearing failure modes can be calculated as the ratio of the top and bottom cold-formed steel thickness (t_2/t_1). For $t_2/t_1 \leq 1$, the nominal shear strength is taken as the smaller of tilting failure mode (Eq. (1.1)) and bearing failure mode (Eqs (1.2) and (1.3)). For $t_2/t_1 \geq 2.5$, the nominal shear strength is taken as the smaller of Eqs (1.2) and (1.3). For $1 \leq t_2/t_1 \geq 2.5$, the nominal shear strength is calculated by linear interpolation between the above two cases:

$$(1.1) \qquad\qquad P_{ns} = 4.2\sqrt{t_2^3 d F_{u,2}},$$

$$(1.2) \qquad\qquad P_{ns} = 2.7 t_2 d F_{u,2},$$

$$(1.3) \qquad\qquad P_{ns} = 2.7 t_1 d F_{u,1}.$$

In a bearing failure, the screws remain perpendicular to the cold-formed steel plate with a longitudinal tear forming a failure zone in front of the screw. For a tilting failure, the screw connection fails due to the eccentric shear load placed on the screw by the two connection plates which affects the rotation of the screw. The tilting or the rotation of the screw effects the pull-out failure modes when the rotation deformation is large [17]. In practical design, the structural engineer cannot predict the actual screw rotation force. This predictive uncertainty impacts the selection of the design equation for either bearing failure and tilting failure. To overcome this uncertainty, it is suggested that the rotation deformation of the screw should be used to identify screw connection behavior in terms of bearing or tilting failure.

This study developed a method of analysis for determining the screw rotation in a single lap screw connection. The screw connection specimens included

a single screw, a double screw, and a quadruple screw connection. The test results were compared with finite element analysis (FEA). The screw rotation in a single lap screw connection was analyzed by the analytical method, applying the spring model and a screw-plate stiffness equation. The proposed screw-plate stiffness equation was verified by the results of the experimental test and FEA, and the parametric study method using the spring model and screw-plate stiffness was used to study the screw rotation with varying screw thread diameters, plate thicknesses, and plate thickness ratios.

2. EXPERIMENTAL TEST AND FINITE ELEMENT ANALYSIS

The specimen screws were tested using the universal testing machine in the structural laboratory at Kasetsart University, Thailand. The tests were to study the shear strength capacity and load-deformation behavior of screw connections. The cold-formed steel plate used was 1.0 mm thickness with a coating material composed of 55% aluminum, 43.5% zinc, and 1.5% silicon. The material properties of the cold-formed steel and screws; yield strength, ultimate strength, and modulus of elasticity, are presented in Tables 1 and 2, which follow the ASTM standard.

Table 1. Material properties of cold-formed steel, G550.

	Test No.					Mean	SD	COV
	CT-1	CT-2	CT-3	CT-4	CT-5			
t [mm]	1.045	1.045	1.044	1.045	1.045	1.045	0.0004	0.04
w [mm]	12.64	12.65	12.59	12.58	12.52	12.59	0.0522	0.41
F_y [MPa]	608.5	605.80	605.9	617.5	606.5	608.8	4.97	0.81
F_u [MPa]	627.0	622.5	625.5	630.0	620.0	625.0	3.89	0.62
E [GPa]	213.51	213.49	213.49	213.58	213.58	213.53	44.18	0.02
F_u/F_y	1.03	1.02	1.03	1.02	1.02	1.02	0.0054	0.53

Remark: A370-07b standard test methods and definitions for mechanical testing of steel products [18].

Table 2. Material properties of screw.

	Test No.					Mean	SD	COV
	ST-1	ST-2	ST-3	ST-4	ST-5			
d [mm]	4.87	4.89	4.89	4.88	4.82	4.87	0.029	0.599
F_y [MPa]	762.00	754.00	761.00	765.00	758.00	760	4.183	0.486
F_u [MPa]	823	821	826	819	813	820.4	4.879	0.530
E [GPa]	204.082	204.086	204.081	204.079	204.081	204.082	7.385	0.004

Remark: ASTM C1513-18 standard specifications for steel tapping screws for cold-formed steel framing Connections [19].

The three specimen screw configurations are illustrated in Fig. 1. According to the AISI standard [16], the minimum spacing recommended is not less than three times the screw thread diameter (d). In practical terms, the screw spacing was more $3 \times d$ because it was easier to work with this spacing. This screw spacing is common as a working practice in Thailand. The screw connection was assembled by hand tightening with low pre-stress created between the interfaces of the cold-formed steel plates. The labeling of the specimens is S-n, D-n, and Q-n, where the first letter indicates the connection type (S is a single screw connection, D is a double screw connection, and Q is a quadruple screw connection), while the second letter (n) specifies the number of the repeated test.
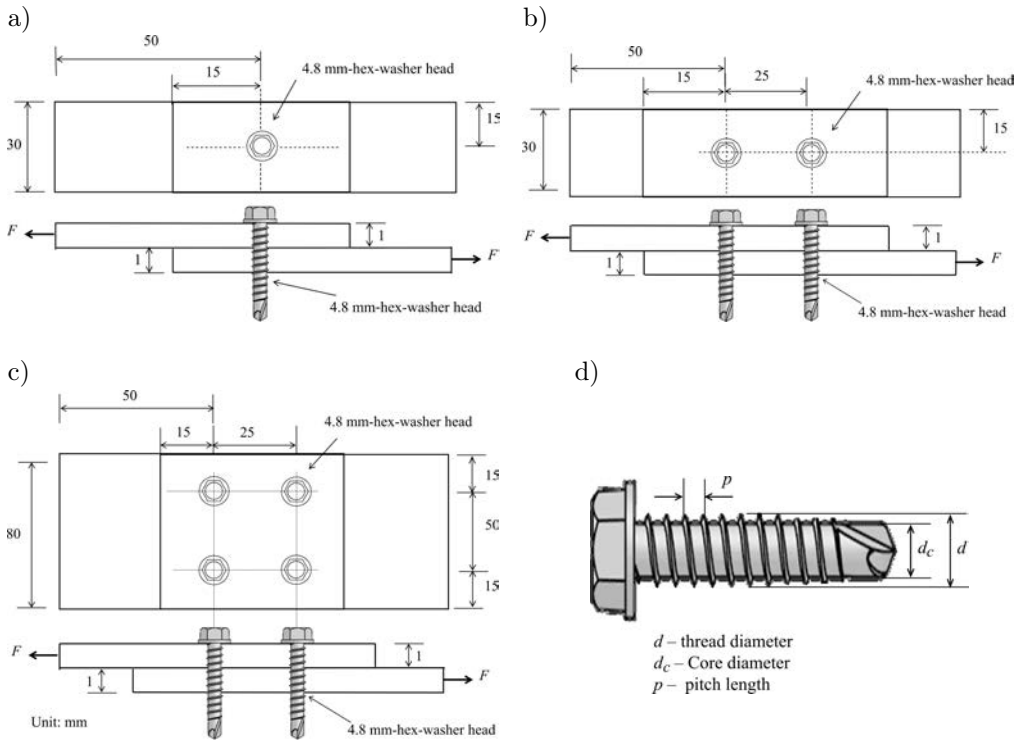

FIG. 1. Screw connection specimens: a) single screw connection, b) double screw connection, c) quadruple screw connections, d) screw dimension.

The screw connections were set up on the universal testing machine (Fig. 2). The load was applied to the specimen using a displacement control with a speed of 1 mm/minute. The displacement of the specimen was measured using a linear variable differential transformer (LVDT). It was installed to operate the elongation of screw connection over a distance from the center line (fixed gauge length). The fixed gauge length for a single screw, double screw and quadruple screw was

Fig. 2. Screw connection test setup: a) test apparatus, b) test specimen.
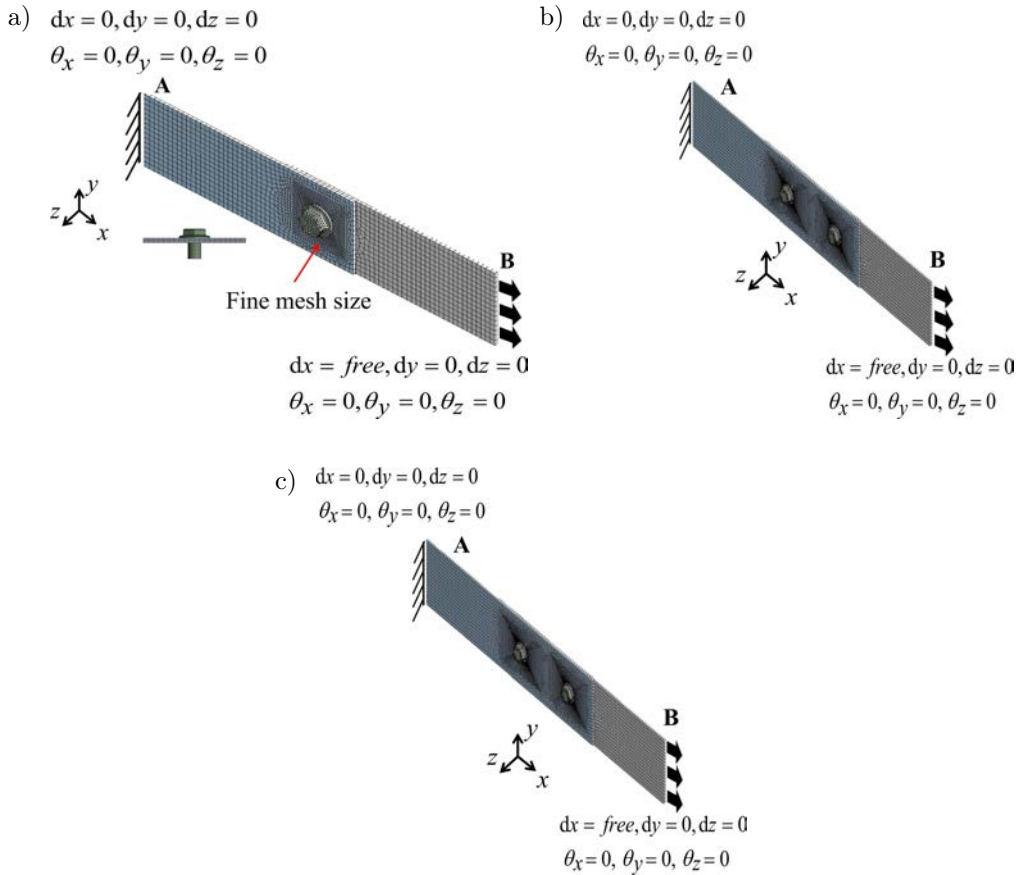

Fig. 3. Geometric model of finite element model: a) single screw connection, b) double screw connection, c) quadruple screw connections.

40, 80, and 80 mm, respectively. LVDT and load cell were linked to the data logger with computer monitoring, and the data was sampled at 1.0 s intervals. The connection was considered as having failed when the specimen entered into a plastic deformation state. When the applied force began to drop the test was stopped, even though the specimen continued to elongate.

The ANSYS finite element program [20] was used to investigate the behavior of the screw connection. The material non-linearity, large deformation and contact problems were included in the finite element procedure. In the geometric model, the connection geometry and loading conditions related to the experimental test, was conducted on the finite element model except for the screw thread (Fig. 3). Using the screw geometry model without the screw thread saves CPU and process time [21].

The SHELL181 element, being a flat element, is adequate for the computation of the nonlinear behavior of both thin and moderately thick shell structures and was therefore used in the cold-formed steel plate modeling (Fig. 4a) and was subjected to simultaneous bending stresses and membrane stresses. SOLID186 was used for the screw element (Fig. 4b). The plate to plate and plate to screw shaft interactions between the materials were modeled by the
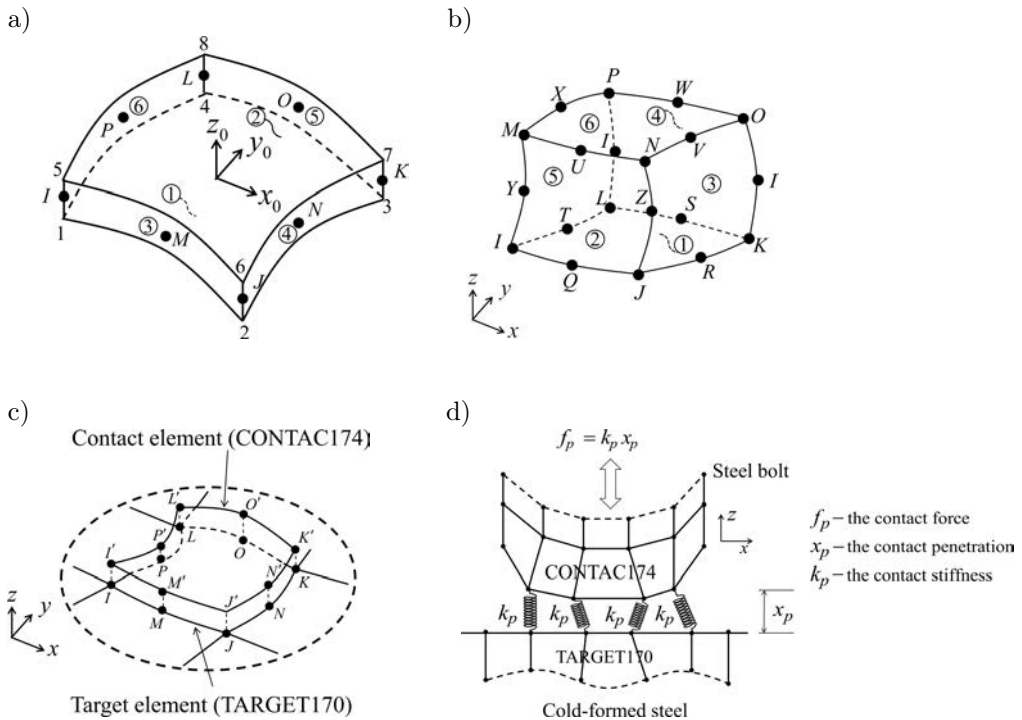

FIG. 4. Element type of finite element model: a) SHELL 181, b) SOLID186, c) CONTAC174 and TARGET170, d) penalty algorithm.

CONTAC174 and TARGET170 (Fig. 4c). The bonded contact pair, frictional contact pair, and the penalty algorithm (Fig. 4d), were provided for the approximate solution of the contact problem. The user-defined coefficient of friction was set at 0.20 [22].

Element aspect ratios were designated to be close to 1.0 for both the shell and solid elements mesh size. Finer mesh was positioned around the hole to transfer the stress from the screw to the cold-formed steel. The stress (σ_{test}) and strain ($\varepsilon_{\text{test}}$) results of the material properties tests were converted to true stress (σ_{true}) and strain ($\varepsilon_{\text{true}}$) curves by Eq. (2.1) and were placed into the multi-linear isotropic hardening material model

$$(2.1) \qquad \sigma_{\text{true}} = \sigma_{\text{test}} \left(1 + \varepsilon_{\text{test}}\right) \qquad \text{and} \qquad \varepsilon_{\text{true}} = \ln\left(1 + \varepsilon_{\text{test}}\right).$$

For boundary and loading conditions, the ends of the two connected plate were restrained using geometric boundary conditions as pinned and roller support. Uniform displacement was applied to the roller support along the positive X direction with a maximum increment for each step of approximately 0.5 mm/step. The load in the FEA model was measured by integrating all x-components of the support reaction. The Newton-Raphson Procedure with the adaptive descent technique (NROPT), the line search option (LNSRCH), and the arc-length method (ARCLEN), were used to obtain the non-linear solution after each displacement increment [20].

3. Results

The load-deformation curve of the experimental test and finite element analysis are presented in the same curve (Fig. 5).

For each of the curves, the linear elastic behavior presented at the beginning until the plastic behavior formed in the screw hole and appeared to be the maximum load. Increasing the number of screws in the connection effected the connection strength, which increased. The failure mode of the specimens exhibited similar failure behavior between the single and multi-screw connection. The maximum load was identified by the bearing failure mode and the specimen was distorted by tilting failure mode. However, some of the screws in the multi-screw connection specimens sheared off, but this only occured after the ultimate load was achieved and the specimens were tested to destruction. The ratio of the ultimate loads between the experiment and the FEA ($P_{\text{test}}/P_{\text{FEA}}$) indicates that the experimental results were in good correlation with the FEA. In P_{test}/P_{ns}, the nominal shear strengths of AISI-2015 [16] were lower than the test results which is conservative for the screw connection design (Table 3).
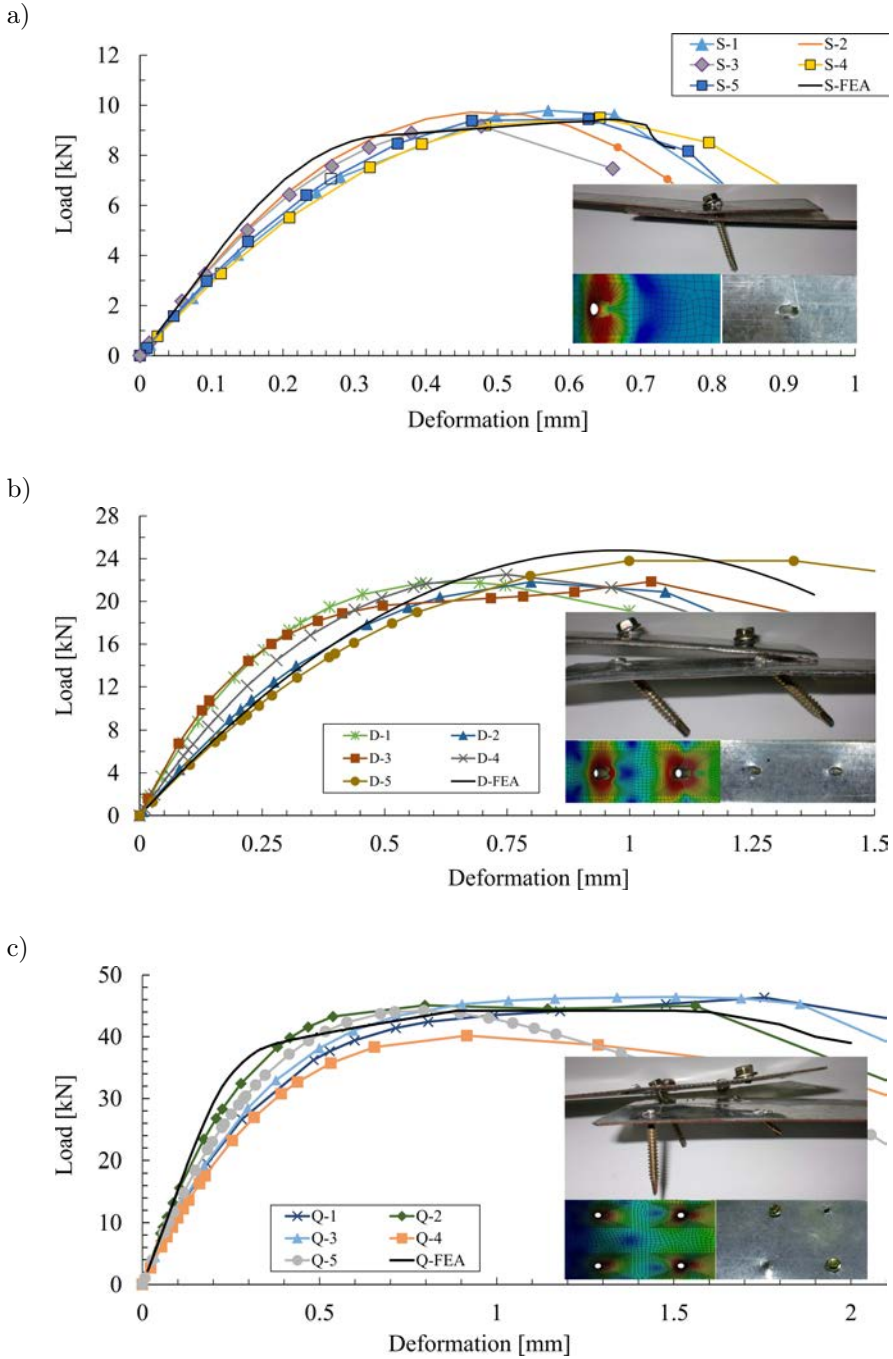
a)

b)

c)

Fig. 5. Load-deformation curve and deformation shape of the screw connections:
a) single screw connection, b) double screw connection, and
c) quadruple screw connections.

Table 3. Summarization of the lap shear connection results.

Test	Loading capacity [kN]	Failure mode	$P_{\text{test}}/P_{\text{FEA}}$	P_{test}/P_{ns}
Single screw connection				
SS-1	9.795	B+T	1.04	1.00
SS-2	9.727	B	1.03	0.99
SS-3	9.170	B	0.97	0.94
SS-4	9.504	B	1.01	0.97
SS-5	9.450	B	1.00	0.96
Mean	9.529		1.01	0.97
COV	2.602			
FEA	9.439	T		
AISI-2015				8.100
Double screw connection				
DS-1	21.743	B+T + S(1 screw shear off)	0.88	1.34
DS-2	21.811	B+T	0.88	1.35
DS-3	21.860	B+T	0.88	1.35
DS-4	22.510	B+T +S (1 screw shear off)	0.91	1.39
DS-5	23.801	B+T +S (2 screw shear off)	0.96	1.47
Mean	22.345		0.90	1.38
COV	3.896			
FEM	24.775	B		
AISI-2015				16.200
Quadruple screw connection				
QS-1	46.358	B+T+S (2 screw shear off)	1.05	1.43
QS-2	45.085	B+T+S (2 screw shear off)	1.02	1.39
QS-3	46.430	B+T	1.05	1.43
QS-4	40.173	B+T+S (2 screw shear off)	0.91	1.24
QS-5	44.213	B+T +S (3 screw shear off)	1.00	1.36
Mean	44.452		1.00	1.37
COV	5.770			
FEA	44.240	B		

Note: B = Bearing, T = Tilting, and S = Screw shear.

4. Screw-plate stiffness analysis

Hook's Law assumptions were used in Eq. (4.1) to predict the screw stiffness. The applied force on the screw connection (F_s) was analyzed with an uninformed load relationship by Eq. (4.2). The deformation of the screw (δ_s) was analyzed

at the reference points A, B, and C. These points represent the location at the middle of the plate thickness and screw (Fig. 6)

$$(4.1) \qquad\qquad F_s = k_s \delta_s,$$

where k_s is the stiffness of the screw

$$F_s = \omega_1 t_1 = \omega_2 t_2,$$

$$(4.2)$$
$$\omega_1 = \omega_2 \left(\frac{t_2}{t_1} \right),$$

where t_1 and t_2 are the thickness of the plate, ω_1 and ω_2 are the loads on the screw.
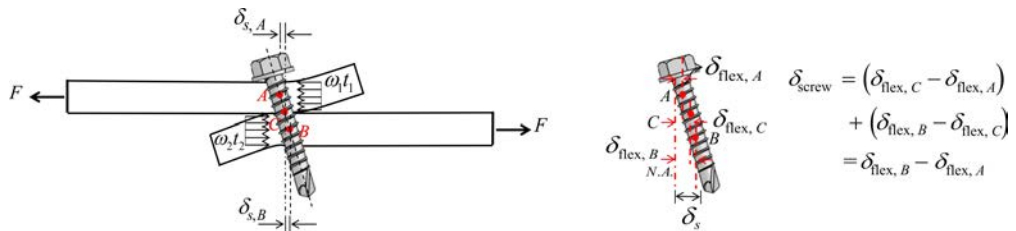

FIG. 6. Single screw connection model.

The deformation of the screw due to the partially uniform bearing load (Fig. 7a) was analyzed by the statically determinate system as a cantilever beam with partially uniform loads (Fig. 7b). The deformation at point A and point B were calculated by using the principle of superposition (Fig. 8).
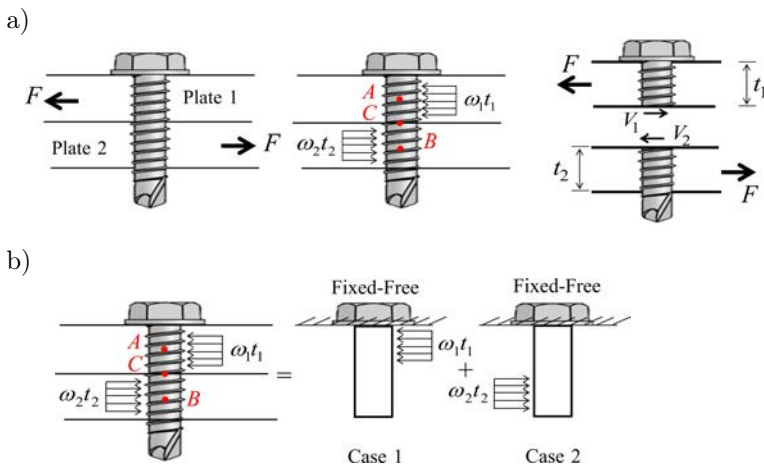

FIG. 7. Load condition in the single-lap connection: a) the force diagram of the screw connection, b) statically determinate system.
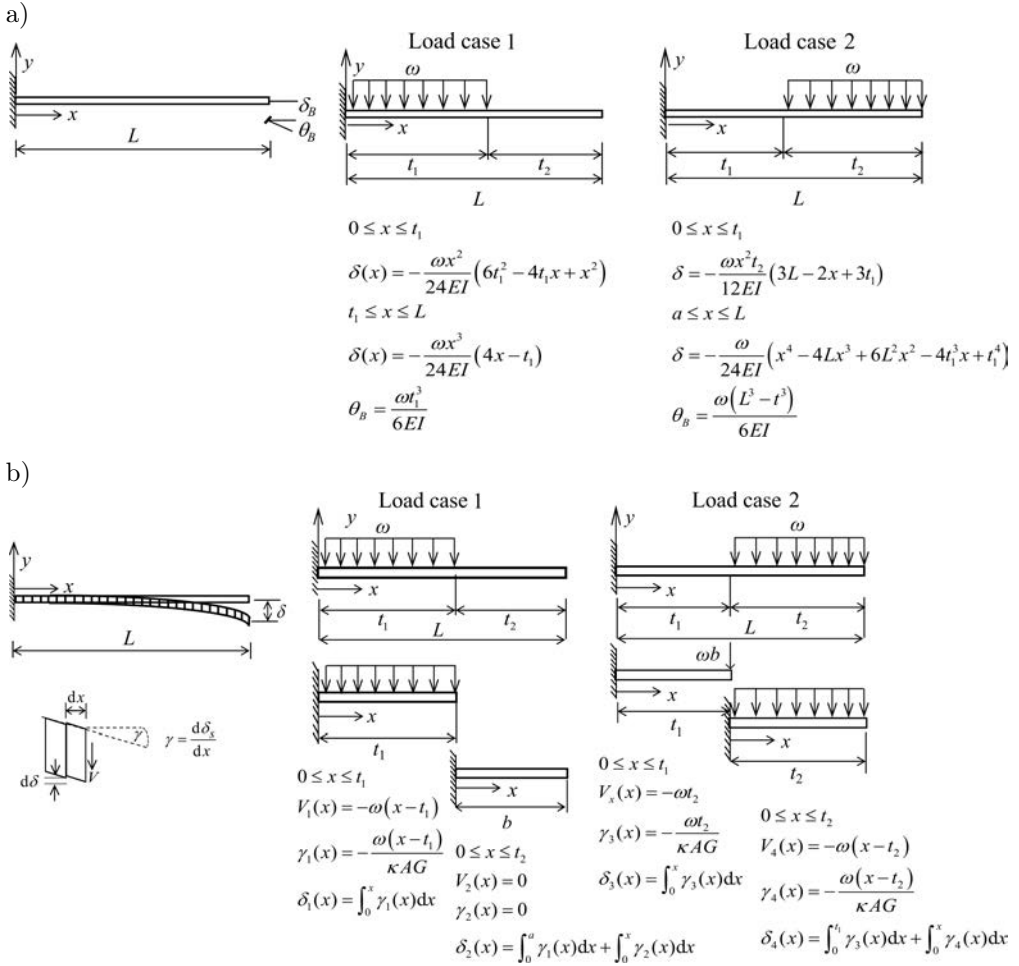
a)

b)

FIG. 8. Deformation of a cantilever beam: a) bending deformation, b) shear deformation.

For screw bending stiffness, displacements of point A ($\delta_{\text{flex},A}$) caused by $\omega_1 t_1$ and $\omega_2 t_2$ are calculated by Eqs (4.3)

$$\delta_{\text{flex},A} = \delta_{\text{flex},A,\omega_1 t_1} + \delta_{\text{flex},A,\omega_2 t_2},$$

$$\delta_{\text{flex},A,w_1 t_1} = -\frac{\omega_1 t_1^3}{24 E_s I_s} \left(6a^2 - 4ax + x^2\right),$$

(4.3)

$$\delta_{\text{flex},A,w_2 t_2} = \frac{\omega_2 b x^2}{12 E_s I_s} \left(3L + 3a - 2x\right),$$

$$a = t_1, \qquad b = t_2, \qquad L = t_1 + t_2, \qquad \text{and} \qquad x = \frac{t_1}{2},$$

where $\delta_{\text{flex},A,w_1t_1}$ and $\delta_{\text{flex},A,w_2t_2}$ are the flexural deformation at point A due to ω_1t_1 and ω_2t_2, E_s is the modulus of elasticity of the screw, I_s is the moment of inertia of the screw, and L is the length of the screw.

Displacements of point B ($\delta_{\text{flex},B}$) caused by ω_1t_1 and ω_2t_2 are calculated by Eqs (4.4)

$$\delta_{\text{flex},B} = \delta_{flex,B,\omega_1t_1} + \delta_{\text{flex},B,\omega_2t_2},$$

(4.4)
$$\delta_{\text{flex},B,\omega_1t_1} = -\frac{\omega_1a^3}{24E_sI_s}\left(4x - a\right),$$

$$\delta_{\text{flex},B,\omega_2t_2} = \frac{\omega_2}{24E_sI_s}\left(x^4 - 4Lx^3 + 6L^2x^2 - 4a^3x + a^4\right),$$

$$x = t_1 + \frac{t_2}{2},$$

where $\delta_{\text{flex},B,w_1t_1}$ and $\delta_{\text{flex},B,w_2t_2}$ are the flexural deformations at point B due to ω_1t_1 and ω_2t_2.

The screw flexural deformation (δ_{flex}) due to ω_1t_1 and ω_2t_2 is defined by Eq. (4.5)

(4.5) $$\delta_{\text{flex}} = \delta_{\text{flex},B} - \delta_{\text{flex},A} = \frac{1}{384}\frac{\omega_1t_1\left(57t_1^3 + 136t_1^2t_2 + 96t_1t_2^2 + 17t_2^3\right)}{E_sI_s}.$$

The bending stiffness of the screw is defined by Eq. (4.6)

(4.6) $$\frac{1}{k_{\text{flex}}} = \frac{\delta_{\text{flex}}}{F_s} = \frac{\left(57t_1^3 + 136t_1^2t_2 + 96t_1t_2^2 + 17t_2^3\right)}{384E_sI_s}.$$

For shear stiffness, displacements of point A ($\delta_{sh,A}$) caused by ω_1t_1 and ω_2t_2 are calculated by Eq. (4.7)

$$\delta_{sh,A} = \delta_{sh,A,\omega_1t_1} + \delta_{sh,A,\omega_2t_2},$$

(4.7)
$$\delta_{sh,A,w_1t_1} = \int_0^x \gamma_1(x)\,\mathrm{d}x = -\frac{3\omega_1t_1^2}{8\kappa G_sA_s},$$

$$\delta_{sh,A,w_2t_2} = \int_0^x \gamma_3(x)\,\mathrm{d}x = \frac{\omega_2t_1t_2}{2\kappa G_sA_s},$$

$$x = \frac{t_1}{2},$$

where δ_{sh,A,w_1t_1} and δ_{sh,A,w_2t_2} are the shear deformations at point A due to ω_1t_1 and ω_2t_2, A_s is the cross-sectional area of the screw and G_s is the shear modulus of the screw κ is the shear coefficient is 0.93 [23].

For shear stiffness, displacements of point B ($\delta_{sh,B}$) caused by $\omega_1 t_1$ and $\omega_2 t_2$ are calculated by Eqs (4.8)

$$\delta_{sh,B} = \delta_{sh,B,\omega_1 t_1} + \delta_{sh,B,\omega_2 t_2},$$

(4.8)
$$\delta_{sh,B,w_1 t_1} = \int_0^a \gamma_1(x)\,\mathrm{d}x + \int_0^x \gamma_2(x)\,\mathrm{d}x = -\frac{\omega_1 t_1^2}{2\kappa G_s A_s},$$

$$\delta_{sh,B,w_2 t_2} = \int_0^a \gamma_3(x)\,\mathrm{d}x + \int_0^x \gamma_4(x)\,\mathrm{d}x = \frac{\omega_2 t_2 (8t_1 + 3t_2)}{8\kappa G_s A_s},$$

$$x = \frac{t_2}{2},$$

where $\delta_{sh,B,w_1 t_1}$ and $\delta_{sh,B,w_2 t_2}$ are the shear deformation at point B due to $\omega_1 t_1$ and $\omega_2 t_2$.

The screw shear deformation (δ_{sh}) due to $\omega_1 t_1$ and $\omega_2 t_2$ is defined by Eq. $(4.9)_1$, and the shear stiffness of the screw is defined by Eq. $(4.9)_2$:

(4.9)
$$\delta_{sh} = \delta_{sh,B} - \delta_{sh,A} = \frac{3}{8}\left(\frac{t_1 + t_2}{\kappa A_s G_s}\right)\omega_2 t_2,$$

$$\frac{1}{k_{sh}} = \frac{\delta_{sh}}{F_s} = \frac{3(t_1 + t_2)}{8\kappa A_s G_s}.$$

The bearing stiffness of the screw and the plate are calculated by using the schematic diagram of bearing stiffness (Fig. 9). The bearing stiffness of the screw ($k_{\mathrm{bea},s}$) and plate ($k_{\mathrm{bea},p}$) are defined by Eqs (4.10).

(4.10)
$$\frac{1}{k_{\mathrm{bea},s}} = \frac{1}{t_1 E_s} + \frac{1}{t_2 E_s},$$

$$\frac{1}{k_{\mathrm{bea},p}} = \frac{1}{t_1 E_{p,1}} + \frac{1}{t_2 E_{p,2}},$$

where σ_{bea} is bearing stress, $\varepsilon_{\mathrm{bea}}$ is bearing strain, P is the applied load, $E_{p,1}$ and $E_{p,2}$ is the modulus of elasticity of plate 1 and plate 2.

All stiffness values were combined to be the screw-plate stiffness as proposed by Eq. (4.11)

(4.11)
$$\frac{1}{k_{sp}} = \frac{57t_1^3 + 136t_1^2 t_2 + 96t_1 t_2^2 + 17t_2^3}{384 E_s I_s} + \frac{3}{8}\frac{(t_1 + t_2)}{\kappa A_s G_s}$$

$$+ \left(\frac{1}{t_1 E_s} + \frac{1}{t_2 E_s}\right) + \left(\frac{1}{t_1 E_{p1}} + \frac{1}{t_2 E_{p2}}\right).$$
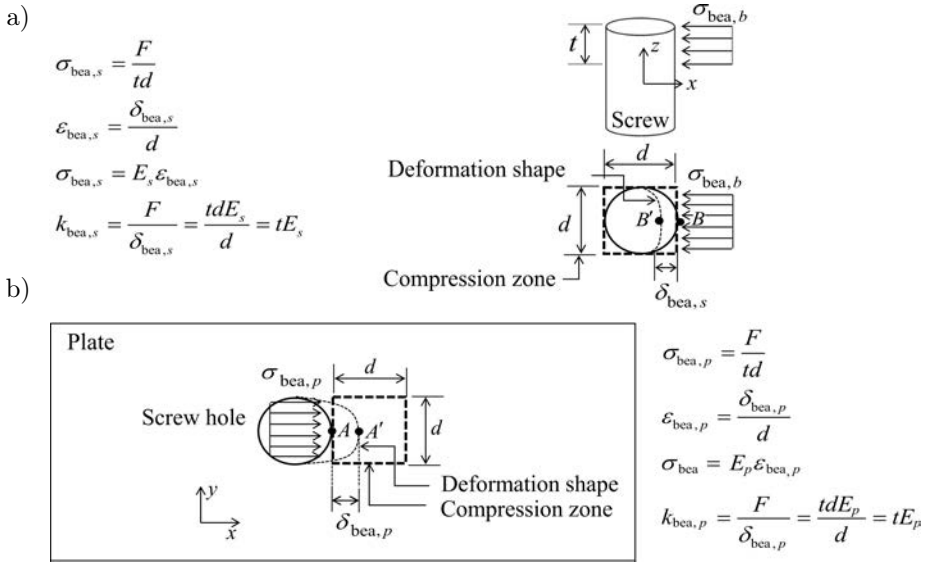
a)

b)

FIG. 9. The schematic diagram of bearing stiffness: a) bearing stiffness for the screw,
b) bearing stiffness for the plate.

The analytical model related the single screw connection specimen was idealized as a spring model (Fig. 10) to verify the accuracy of the screw-plate stiffness equation. The stiffness of components in Table 4 was written by the matrix equation as Eq. (4.12) [24],
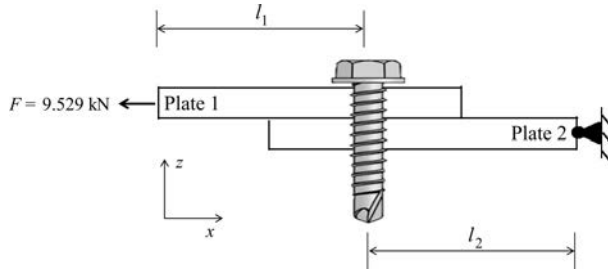
$$
(4.12) \qquad
\left\{ \begin{array}{c} 0 \\ 0 \\ F_3 \end{array} \right\}
=
\left[\begin{array}{ccc}
k_{sp} + k_{p-2} & -k_{sp} & 0 \\
-k_{sp} & k_{sp} + k_{p-1} & -k_{p-1} \\
0 & -k_{p-1} & k_{p-1}
\end{array} \right]
\left\{ \begin{array}{c} u_1 \\ u_2 \\ u_3 \end{array} \right\}.
$$

Table 4. Plate stiffness.

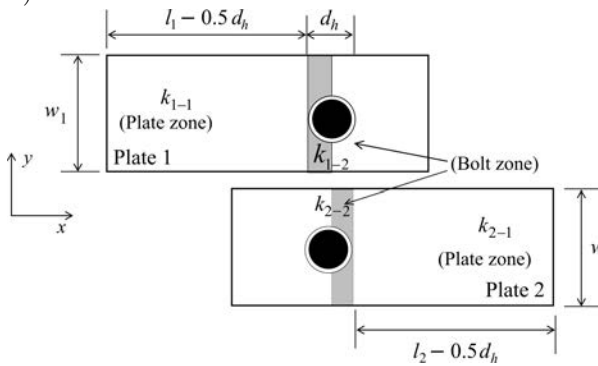| Stiffness	Stiffness equation
$\dfrac{1}{k_{p,1}}$	$\dfrac{1}{k_{1-1}} + \dfrac{1}{k_{1-2}} = \dfrac{1}{\frac{w_1 t_1 E_{p1}}{(l_1 - 0.5 d_h)}} + \dfrac{1}{\frac{(w_1 - d) t_1 E_{p1}}{0.5 d_h}}$
$\dfrac{1}{k_{p,2}}$	$\dfrac{1}{k_{2-1}} + \dfrac{1}{k_{2-2}} = \dfrac{1}{\frac{(w_2 - d) t_2 E_{p2}}{0.5 d_h}} + \dfrac{1}{\frac{w_2 t_2 E_{p2}}{(l_2 - 0.5 d_h)}}$
$\dfrac{1}{k_{sp}}$	$\dfrac{57 t_1^3 + 136 t_1^2 t_2 + 96 t_1 t_2^2 + 17 t_2^3}{384 E_s I_s} + \dfrac{3}{8} \dfrac{(t_1 + t_2)}{\kappa A_s G_s} + \left(\dfrac{1}{t_1 E_s} + \dfrac{1}{t_2 E_s} \right) + \left(\dfrac{1}{t_1 E_{p1}} + \dfrac{1}{t_2 E_{p2}} \right)$

Remark: $k_{p,1}$ and $k_{p,2}$ are the plate stiffness and $E_{p,1}$ and $E_{p,2}$ are the modulus of elasticity of plate 1 and plate 2.

a)

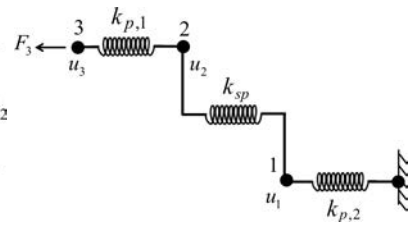b)   c)

FIG. 10. Spring model of single-lap screw connections: a) single-lap two-screw connection,
b) connection stiffness, c) spring model.

The analytical results show that the spring model of single screw connection model was in good correlation with the FEA and the experimental results (Fig. 11).
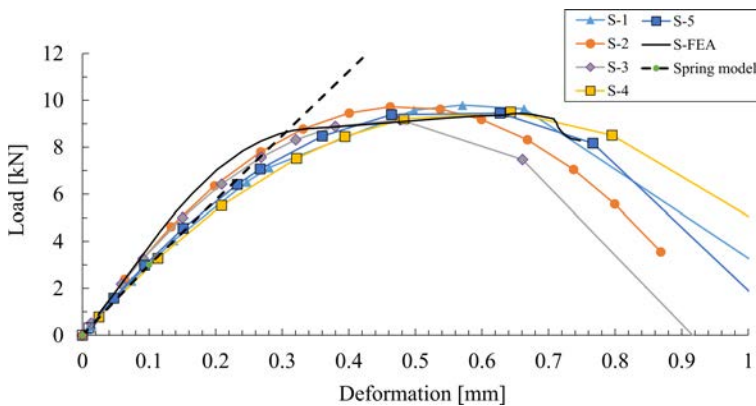

FIG. 11. Comparison of spring model with the FEA and the experimental results.

5. SCREW ROTATION PARAMETRIC STUDY

In previous research [25], the screw-fastened cold-formed steel-to-steel shear connections were investigated by the experimental test. The results show that the tilting failure mode occurred when the fastener tilts were higher than $10°$ and introduced the potential for screw pullout from the cold-formed steel plate. Thus, the proposed analytical method can be applied in the determination of screw rotation in cold-formed steel connections and in a study of the effects of the geometry parameters on screw rotation (θ).

In the parametric study, variations in the screw thread diameter (d), plate thickness ($t = t_1 = t_2$) and plate thickness ratio (t-ratio $= t_2/t_1$) were assigned to the spring model and were related to the single screw connection specimen for calculating the screw rotation (Fig. 12). The geometry parameters and analysis results were presented in Tables 5–7.
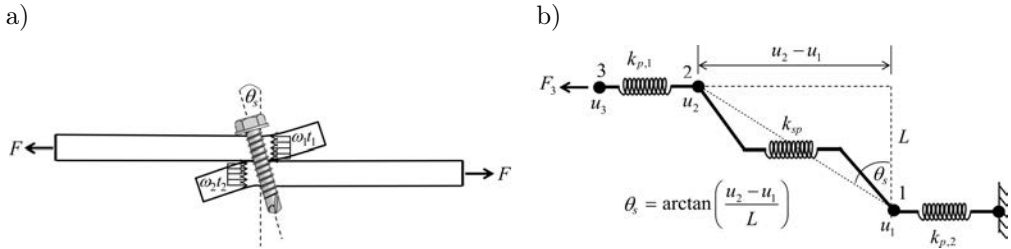

a)

b)

FIG. 12. Single screw connection model for parametric study: a) geometry model, b) spring model for the parametric study.

Table 5. The geometric parameter and analysis results of variations in the screw thread diameter (d).

Case	t_1 [mm]	t_2 [mm]	t_2/t_1	d [mm]	θ [deg.]
1	1.00	1.00	1.00	1.20	8.18
2	1.00	1.00	1.00	2.00	6.56
3	1.00	1.00	1.00	2.50	5.77
4	1.00	1.00	1.00	3.00	5.48
5	1.00	1.00	1.00	4.00	5.30
6	1.00	1.00	1.00	5.00	5.25
7	1.00	1.00	1.00	6.00	5.23
8	1.00	1.00	1.00	8.00	5.22
9	1.00	1.00	1.00	10.00	5.22
10	1.00	1.00	1.00	12.00	5.22

Table 6. The geometric parameter and analysis results of variations
in the plate thickness ($t_1 = t_2$).

Case	t_1 [mm]	t_2 [mm]	t_2/t_1	d [mm]	θ [deg.]
1	0.20	0.20	1.00	5.00	66.35
2	0.40	0.40	1.00	5.00	29.72
3	0.60	0.60	1.00	5.00	14.25
4	0.80	0.80	1.00	5.00	8.14
5	1.00	1.00	1.00	5.00	5.25
6	1.20	1.20	1.00	5.00	3.68
7	1.40	1.40	1.00	5.00	2.74
8	1.60	1.60	1.00	5.00	2.13
9	1.80	1.80	1.00	5.00	1.73
10	2.00	2.00	1.00	5.00	1.45

Table 7. The geometric parameter and analysis results of variations
in the plate thickness ratio (t_2/t_1).

Case	t_1 [mm]	t_2 [mm]	t_2/t_1	d [mm]	θ [deg.]
1	1.00	1.00	1.00	5.00	5.25
2	1.00	2.00	2.00	5.00	2.68
3	1.00	3.00	3.00	5.00	1.84
4	1.00	4.00	4.00	5.00	1.45
5	1.00	5.00	5.00	5.00	1.25
6	1.00	6.00	6.00	5.00	1.13
7	1.00	7.00	7.00	5.00	1.07
8	1.00	8.00	8.00	5.00	1.06
9	1.00	9.00	9.00	5.00	1.07
10	1.00	10.00	10.00	5.00	1.10

The parametric study results showed that the rotation of the screw decreased when the screw thread diameter increased (Fig. 13a). The change of the screw thread diameter affects the screw-plate stiffness between the screw and the plates which results in the screw and plate deformations.

Changing the screw thread diameter has little impact on the fastener tilts. The failure mode was constrained by the bearing failure mode when the fastener tilt rotation values are less than 10°. High rotation results were presented in the analysis case by varying plate thickness (Fig. 13b). The bending stiffness was lost due to decreased plate thickness which resulted in screw rotation increasing,
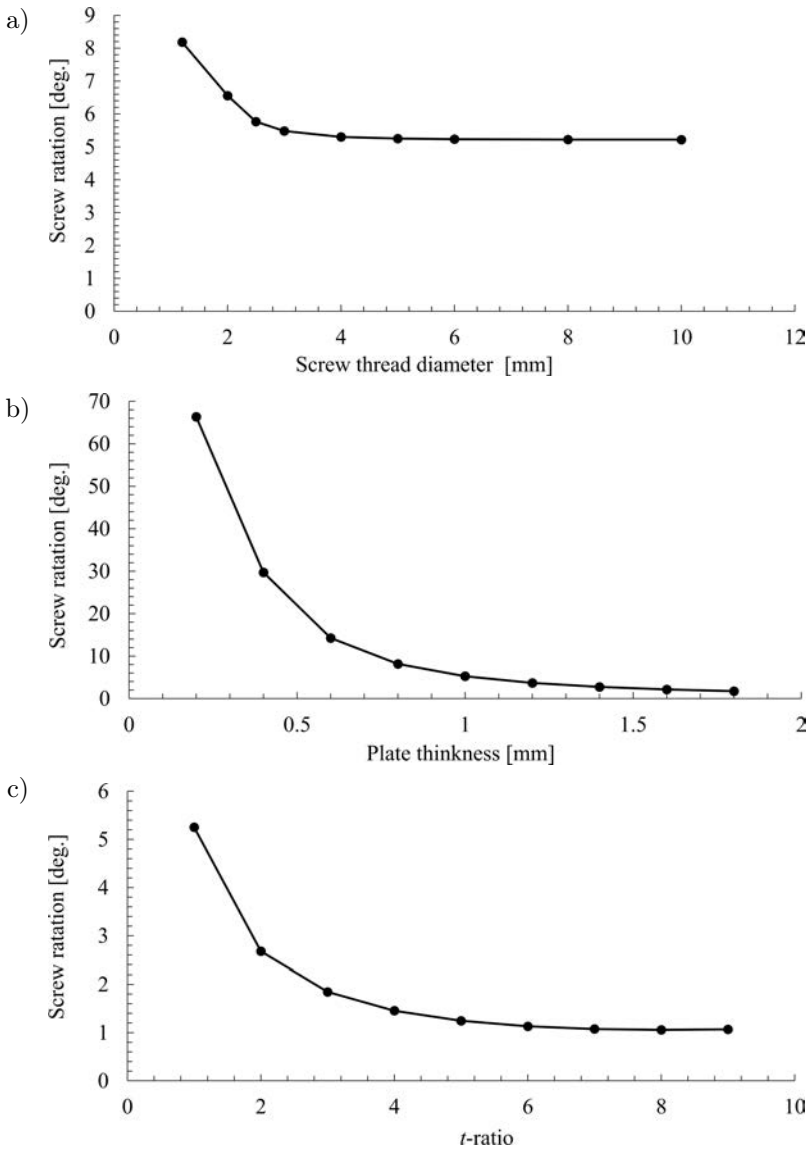
a)

b)

c)

FIG. 13. Parametric study: a) rotation results of varying screw thread diameters, Case-A, b) rotation results of varying plate thickness, c) rotation results of the plate thickness t-ratio.

as the thin plate cannot resist the secondary bending moment due to a shearing force couple which resulted in screw tilting.

As shown in Fig. 13c, the screw rotation decreased when t-ratio increased. While the t_2/t_1 ratio was greater than 1 ($t_2/t_1 \gg 1$), the end of the screw was constrained by the bending stiffness of Plate 2 which had semi-fixed support.

From the results of the parametric study, it can be concluded that the bending stiffness of the plate is a major factor in the control of screw rotation.

6. Conclusion

An experimental test and finite element analysis of screw connections were carried out in order to develop an analytical method for screw rotation study. The screw connections studied included single, double and quadruple screw lap shear tests with a material thickness of 1.0 mm and a screw thread diameter of 4.8 mm. The screw lap shear connection test results were compared with the nominal strength equations given in AISI-2015 [16]. The comparison shows that the nominal strength parameter predicted by AISI-2015 [16] is conservative. Screw rotation and tilting were studied by an analytical method with a spring model. A screw-plate stiffness equation was proposed which included the effect of bending stiffness, shear stiffness and bearing stiffness of both the screws and the cold-formed steel plate. The screw-plate stiffness equation was verified by the FEA and experimental tests, and it is a good correlation with both the FEA and experimental tests. However, the weakness of the developed analytical model was ignoring of the plates deformations caused by secondary bending phenomenon. The parametric study method was used to calculate the rotation of the fastener rotation with variations in the screw thread diameter, plate thickness, and the plate thickness ratio. The results show that the screw rotation is sensitive to plate thickness, and changes significantly with decreased plate thickness. It is also clear that the end of the screw should be embedded within the thickest side of the cold-formed steel parts which then helps protect the tilt of the screw. Our research shows that an analytical method is a successful checking tool for the failure mode of a screw connection, and was used to confirm the failure mode of the design procedure.

Acknowledgment

References

1. Dawe J.L., Liu Y., Li J.Y., *Strength and behaviour of cold-formed steel offset trusses*, Journal of Constructional Steel Research, **66**: 556–565, 2010.

2. VISHNUVARDHAN S., SAMUEL G.M., *Knight behaviour of cold-formed steel single and compound plain angles in compression*, Advanced Steel Construction, **4**(1): 46–58, 2008.

3. KLIPPSTEIN K.H., *Strength of cold-formed steel studs exposed to fire*, Proceedings of the 4th international specialty conference on cold-formed steel structures, University of Missouri-Rolla, pp. 513–55, 1978.

4. KLIPPSTEIN K.H., *Behaviour of cold-formed steel studs in fire tests*, Proceedings of the 5th international specialty conference on cold-formed steel structures, University of Missouri-Rolla, pp. 275–300, 1980.

5. HANCOCK G.J., *Cold-formed steel structures*, Journal of Constructional Steel Research, **56**(4): 473–487, 2003.

6. LEE Y.H., TAN C.S., MOHAMMAD S., TAHIR M.M., SHEK P.N., *Review on cold-formed steel connections*, The Scientific World Journal, **2014**, Article ID 951216, 11 pages, 2014, https://doi.org/10.1155/2014/951216.

7. SHAH S.N.R., SULONG-RAMLI N.H., KHAN R., JUMAAT M.Z., *Structural performance of boltless beam end connectors*, Advanced Steel Construction, **13**(2): 144–159, 2017.

8. MILLS J., LABOUBE R., *Self-drilling screw joints for cold formed channel portal frames*, Journal of Structural Engineering, **130**(11): 1799–1806, 2004.

9. TOMA A., SEDLACEK G., WEYNAND K., *Connections in cold-formed steel*, Thin-walled structures, **16**(1): 219–237, 1993.

10. ROGERS C.A., HANCOCK G.J., *Bearing design of thin sheet steel screwed connections proceedings of international specialty conference on cold-formed steel structures*, International Specialty Conference on Cold-Formed Steel Structures, 1998, http://scholarsmine.mst.edu/isccss/14iccfsss/14iccfsss-session9/1.

11. ROGER C.A., HANCOCK G.J., *Screwed connection tests of thin G550 and G300 sheet steels*, Journal of Structural Engineering, **125**(2): 128–136, 1999.

12. FIORINO L.G., CORTE D., LANDOLFO R., *Experimental tests on typical screw connections for cold-formed steel housing*, Engineering Structures, **29**: 1761–1773, 2007.

13. SERRETTE R., PEYTON D., *Strength of screw connections in cold-formed steel construction*, Journal of Structural Engineering, **135**(8): 951–958, 2009.

14. YU W.-W., LABOUBE R.A., *Cold-formed steel design*, John Wiley & Sons, Inc., Hoboken, New Jersey 2010, doi: 10.1002/9780470949825.

15. ZEYNALIAN M., SHELLEY A., RONAGH H.R., *An experimental study into the capacity of cold-formed steel truss connections*, Journal of Constructional Steel Research, **127**: 176–186, 2016.

16. American Iron and Steel Institute, North American specification for the design of cold-formed steel structural members, Washington, DC, USA, 2015.

17. ROGERS C.A., HANCOCK G.J., *Screwed connection tests of thin G550 and G300 sheet steels*, Research Report No R761, Department of Civil Engineering, the University of Sydney, AUSTRALIA, 1997.

18. ASTM A370-07b, *Standard Test Methods and Definitions for Mechanical Testing of Steel Products*, American Society for Testing and Materials (ASTM), West Conshohocken, PA., 2007.

19. ASTM C1513, *Standard Specification for Steel Tapping Screws for Cold-Formed Steel Framing Connections*, American Society for Testing and Materials (ASTM), West Conshohocken, PA., 2018.

20. *ANSYS user's manual. Revision 15*, ANSYS, Inc., Canonsburg, PA, USA, 2014.

21. FAN L., RONDAL J., CESCOTTO S., *Finite element modelling of single lap screw connections in steel sheeting under static shear*, Thin-Walled Structures, **27**(9): 165–185, 1997.

22. CHUNG K.F., IP K.H., *A general design rule for bearing failure of bolted connections between cold-formed Steel Strips*, International Specialty Conference on Cold-Formed Steel Structures, Missouri, pp. 593–605, 2000.

23. HUTCHINSON J. R., *Shear coefficients for Timoshenko beam theory*, Journal of Applied Mechanics, **68**(1): 87–92, 2000.

24. LIU X., YANG Y., GAO H., BAO Y., LI R., CHEN L., *Effects of hole-perpendicularity error on joint stiffness of single-lap double-bolt composite joints*, Engineering Transactions, **65**(2): 289–305, 2017.

25. CORNER S.M.W., *Screw-Fastened Cold-Formed Steel-to-Steel Shear Connection Behavior and Models*, Master of Science in Mechanical Engineering, Virginia Polytechnic Institute and State University, 2014.